CONF 861207 - -61

THE PHYSICS OF PHOTONS AND NEUTRONS WITH APPLICATIONS OF DEUTERIUM LABELING METHODS TO POLYMERS

G. D. WIGNALL
National Center for Small-Angle Scattering Research, Oak Ridge National Laboratory, Oak Ridge, Tennessee 37831

CONF-861207--61

DE87 005513

INTRODUCTION

Over the past decade small-angle neutron scattering (SANS), has found numerous applications in the fields of biology, polymer science, physical chemistry, materials science, metallurgy, colloids, and solid state physics. A number of excellent references are available [1-4] which contain basic neutron scattering theory though these text books reflect the origins of the technique and the examples are largely drawn from physics e.g., single crystals, simple liquids, monatomic gases, liquid metals, magnetic materials, etc. In view of the large numbers of nonspecialists who are increasingly using neutron scattering, the need has become apparent for presentations which can provide rapid access to the method without unnecessary detail and mathematical rigor. In the field of polymer science several reviews have been written to meet this need [5-8] including a recent comprehensive survey of neutron scattering studies of polymers [9] to which reference will be made for detailed derivations of the expressions used below. This article, along with others in this volume, is meant to serve as a general introduction to the symposium "Scattering Deformation and Fracture in Polymers," and is intended to aid potential users who have a general scientific background, but no specialist knowledge of scattering, to apply the technique to provide new information in areas of their own particular interests. In view of space limitations, the general theory will be given in the case for neutron scattering and analogies and differences with photon scattering (x-rays) will be pointed out at the appropriate point.

"The submitted manuscript has been authored by a contractor of the U.S. Government under contract No. DE-AC05-84OR21400. Accordingly, the U.S. Government retains a nonexclusive, royalty-free license to publish or reproduce the published form of this contribution, or allow others to do so, for U.S. Government purposes."

ENERGY AND MOMENTUM TRANSFER

Scattering in the context of this article means the deflection of a beam of radiation (neutrons/x-rays, etc.) from its original direction by interaction with the nuclei or electrons of polymer or solvent molecules in a sample. In a scattering experiment a proportion of the incident neutrons is scattered and the remaining fraction is transmitted through the sample. The intensity of the scattered neutrons is measured as a function of the scattering angle and/or energy. The kinetic energy of a typical neutron, wavelength $\lambda = 5.3$ A, is $\sim 4.7 \times 10^{-15}$ ergs or 3 meV [9]. Such energies are very much lower than electromagnetic radiation, and are of the same order as the vibrational and diffusional energies of molecular systems. Exchanges of energy between the particle (neutron) and molecule give rise to inelastic scattering which depends on the dynamics of the system studied. While the angular dependence of the scattering of both x-rays and neutrons is easily measured, the energies of molecular vibrations (~ 3 meV) are much lower than incident photons (~ 10 keV) and thus energy transfers are difficult to detect for x-ray scattering. In contrast, the energy transfers resulting from neutron scattering are easily resolved and permit the elucidation of dynamic processes [9]. Neutrons are thus a unique probe for studying the condensed state in that they simultaneously have both the appropriate wavelength and energy to investigate the structure and dynamics of molecular systems in general (including polymers).

For an incident neutron of wavelength λ_0, and velocity v_0 which is scattered through an angle 2θ in an inelastic process (the scatter angle is defined as θ in the complementary article by R. S. Stein), this results in a

DISTRIBUTION OF THIS DOCUMENT IS UNLIMITED

MASTER

final wavelength of λ and velocity v, and the energy gained by the target (and lost by the neutron) is given by

$$E = \frac{m}{2}(v^2 - v_o^2) = \frac{\hbar^2}{2m}(k^2 - k_o^2) = \hbar\omega \tag{1}$$

where $\underline{k}_o$ and $\underline{k}$ are the initial and final wave vectors ($k = 2\pi/\lambda$). The momentum transfer is:

$$\hbar\,\underline{Q} = \hbar(\underline{k} - \underline{k}_o) \tag{2}$$

$$\hbar\,|\underline{Q}| = \hbar(k^2 + k_o^2 - 2kk_o\cos 2\Theta)^{1/2} \tag{3}$$

If energy is transferred in the scattering process ($\Delta E \neq 0$), the process is termed inelastic. If no energy change takes place ($\Delta E = \hbar\omega = 0$, $\lambda = \lambda_o$), the scattering is termed elastic and

$$|\underline{Q}| = \frac{4\pi}{\lambda}\sin\Theta \quad . \tag{4}$$

If ΔE is small compared to the incident neutron energy ($|\Delta E| \ll E_o$) the scattering is termed quasielastic. Most of the neutron scattering measurements on polymers have involved neutrons scattered at small values of the momentum transfer ($Q \to 0$). This type of measurement is usually referred to as small-angle (rather than small Q) neutron scattering though the terms are equivalent for long wavelengths ($\lambda_o > 0.4$ nm). It is easily seen from equation (4) that for long wavelengths, $Q \to 0$ implies $k \to k_o$ and the scattering is predominantly elastic, as any neutron scattered with a large energy transfer ΔE could not satisfy both energy and momentum conservation at small Q [9]. Small-angle neutron scattering (SANS) experiments give information on the time averaged structure and conformation of polymer molecules and form the bulk of the work described in this Symposium. There has been less work on quasielastic and inelastic processes, though such experiments give valuable information on polymer dynamics [9].

SCATTERING LENGTH AND CROSS SECTION

Scattering theory is usually developed by considering a single atom which is fixed at the origin and hence cannot accept energy from the neutron [1,3,4]. The interaction between the neutron and nucleus is known to be very short ranged ($\sim 10^{-7}$ A) compared to the wavelength of the neutron (~ 5 A). Because of this, it is shown in standard texts [1,3,4] that the scattering can contain only zero angular momentum components. This has the important consequence that the scattering is isotropic for slow neutrons and there is no angle-dependent form factor as in the case of x-rays. Thus if an incident plane wave of neutrons is described by a wave function of unit density

$$\psi_o = e^{ik_oz} \tag{5}$$

the scattered wave from a fixed nucleus will be spherically symmetrical and of the form

$$\psi_1 = -\frac{b}{r}e^{ikr} \tag{6}$$

The quantity b has the dimensions of length and is called the scattering length (defined as a in the complementary article by R. S. Stein). Although the value of b is in principle dependent on the incident neutron energy E_0, the variation for energies normally encountered in neutron scattering studies is negligible, and b may be regarded as real and a (known) constant for a given nucleus (isotope). The scattered neutrons may be envisaged as originating from a sphere, radius r, centered on the nucleus, and using the scattering length we may define [1,3,11,12] a scattering cross section σ for the nucleus by

$$\sigma = \frac{\text{number scattered neutrons/sec}}{\text{incident neutron flux}} \tag{7}$$

and hence the single atom cross section is given [9] by

$$\sigma = 4\pi b^2 \tag{8}$$

It can be seen from equation (8) that σ has the dimensions of area.

To a first approximation the cross section may be regarded as the effective area which the target nucleus presents to the incident beam of neutrons for the elastic scattering process. The above cross section (equation 8) is usually called the bound atom cross section as the nucleus was considered fixed at the origin. Where the atom is free to recoil however, e.g., in the gaseous state, the cross section applicable to this state is called the free atom cross section [9]. The bound atom cross section is generally relevant to polymer studies which are virtually always conducted on samples of macroscopic dimensions in the solid or liquid state.

COHERENT AND INCOHERENT CROSS SECTIONS

The magnitude of b varies from nucleus to nucleus and is typically of the order of 10^{-12} cm. This gives rise to the usual unit for a cross section which is called a barn (10^{-24} cm^2). Unlike the x-ray scattering factor, f, which increases with the atomic number of the atom, there is no general trend throughout the periodic table in the values of b, which vary from isotope to isotope and from nucleus to nucleus of the <u>same</u> isotope if it has nonzero spin.

Because the neutron has spin 1/2, it can interact with a nucleus of spin I to form one of two compound nuclei with spins ($I \pm 1/2$), each of which has a different scattering length b^+ and b^- which is associated with the spin up or spin down states. For a given spin state J the number of orientations is (2J+1) and thus the number of possible orientations for the compound spin states of (I+1/2) and (I−1/2) are 2(I+1) and 2 I respectively. The total number of spin states is 2(2I+1) and as the probabilities of each state are equal, the statistical weights are $\frac{I+1}{(2I+1)}$ and $\frac{I}{(2I+1)}$, respectively.

The average (coherent) scattering length is

$$\langle b \rangle = \frac{I+1}{2I+1} b^+ + \frac{I}{2I+1} b^- \tag{9}$$

where the brackets <> represent a thermal average over the spin state population. We may define a coherent cross section for each isotope by

$$\sigma_{coh} = 4\pi\langle b\rangle^2 \tag{10}$$

whereas the total scattering cross section is given by

$$\sigma_{tot} = 4\pi\langle b^2\rangle \tag{11}$$

The difference between the two is the incoherent cross section σ_{inc} which is given by

$$\sigma_{tot} - \sigma_{coh} = \sigma_{inc} = 4\pi\left[\langle b^2\rangle - \langle b\rangle^2\right] \tag{12}$$

If the isotope has no spin then $\langle b^2\rangle = \langle b\rangle^2$ as $\langle b\rangle = b$ and there is no incoherent scattering. Only the coherent scattering cross-section contains information on interference effects arising from spatial correlations of the nuclei in the system i.e., the structure of the sample. The incoherent cross-section contains no information on interference effects and forms an isotropic (flat) background which must be subtracted off in SANS structural investigations. It does however contain information on the motion of single atoms (particularly hydrogen) which may be investigated via energy analysis of the scattered beam [9]. While most of the atoms encountered in neutron scattering from polymers are mainly coherent scatterers (e.g., carbon, oxygen), there is one important exception. In the case of hydrogen (H^1) the spin-up and spin-down scattering lengths have opposite sign ($b^+ = 1.080 \times 10^{-12}$ cm; $b^- = -4.737\ 10^{-12}$ cm), and as $I = 1/2$ we have

$$\sigma_{coh} = 1.76 \times 10^{-24}\ \mathrm{cm}^2 \tag{13}$$

$$\sigma_{tot} = 81.5 \times 10^{-24}\ \mathrm{cm}^2 \tag{14}$$

$$\sigma_{inc} = 79.7 \times 10^{-24}\ \mathrm{cm}^2 \tag{15}$$

For photons, there is no strict analog of incoherent scattering of neutrons due to nonzero spin in the scattering nucleus. Compton scattering which occurs for x-rays is similar in that it contains no information on interference effects, i.e., the structure of the sample and forms a background which must be subtracted off. However, to a good first approximation this background goes to zero in the limit $Q \to 0$ and may be neglected in SAXS studies.

Table 1 gives the cross sections and scattering lengths for atoms commonly encountered in synthetic and natural polymers. These cross sections refer to bound protons and neglect inelastic effects arising from interchange of energy with the neutron. For coherent scattering which is a collective effect arising from the interference of scattered waves over a large correlation volume, this approximation is reasonable, especially at low Q where recoil effects are small. However, for incoherent scattering, which depends on the uncorrelated motion of individual atoms, inelastic effects become increasingly important for long wavelength neutrons with the result that the H-incoherent cross section, and hence the sample transmission is a function of both the incident neutron energy and sample temperature [9,15,16]. It may be seen from Table I that there is a large difference in the coherent scattering length between deuterium and hydrogen and that the latter value is actually negative. This arises from a change of phase of the scattered wave and results in a marked difference in scattering power (contrast) between polymer molecules synthesized with deuterium atoms or hydrogen atoms along the chain.

TABLE I. Bound atom scattering lengths and cross sections for typical elements in synthetic and natural polymers

ATOM	NUCLEUS	b_{COH} (10^{-12} cm)	$\sigma_{COH} = 4\pi b^2_{COH}$ (10^{-24} cm^2)	σ_{INC} (10^{-24} cm^2)	$f_{x\text{-}ray}(\theta=0)$ (10^{-12} cm)
HYDROGEN	^1H	- 0.374	1.76	79.7	0.28
DEUTERIUM	^2H (D)	0.667	5.59	2.01	0.28
CARBON	^{12}C	0.665	5.56	0	1.69
NITROGEN	^{14}N	0.930	11.10	0	1.97
OXYGEN	^{16}O	0.580	4.23	0	2.25
FLUORINE	^{19}Fl	0.566	4.03	0	2.53
SILICON	^{28}Si	0.415	2.16	0	3.94
CHLORINE	*Cl	0.958	11.53	5.9	4.74

*Values are for the naturally occurring element and are an average over the mixture of isotopes.

The basic experiment consists of an incident neutron beam, energy E_o, which is scattered by an assembly of sample nuclei into solid angle $d\Omega$ with with energy change dE recorded by a neutron detector. The double differential scattering cross section for unit volume of sample, $d^2\Sigma/d\Omega dE$, is defined as the number of neutrons scattered per second into a solid angle $d\Omega$ with energy change dE, divided by the incident neutron flux (neutrons/sec/unit area). In this text the symbol σ is used to denote the cross section of a single nucleus, whereas the symbol Σ is used for an assembly of nuclei (except where it denotes the standard summation sign). For such an assembly the double differential scattering cross section is given by standard scattering theory [4] as

$$\frac{d^2\Sigma}{d\Omega dE} = \frac{k}{2\pi k_o}\int_{-\infty}^{+\infty} dt \exp(-i\omega t)\langle \sum_{ij} b_i^* b_j \, F_{ij}\,(Q,t)\rangle \tag{16}$$

$$= \frac{k}{k_o}\, S(Q,\omega)$$

where

$$F_{ij}\,(Q,t) = \exp[-i\underline{Q}\cdot\underline{R}_i(0)]\,\exp\,[i\underline{Q}\cdot\underline{R}_j(t)] \tag{17}$$

In equation (16) the symbol * denotes a complex conjugate and <> denotes a thermal average over all configurations of scatterers at position vectors R(t) at time t. S(Q,ω) is called the scattering law or scattering function. Equation (16) may be separated into coherent and incoherent components of the cross section

$$\frac{d^2\Sigma^{coh}}{d\Omega dE} = \frac{k}{2\pi k_o}\int_{-\infty}^{\infty} dt \exp(-i\omega t)\langle \sum_{ij} \langle b_i\rangle * \langle b_j\rangle \, F_{ij}\,(Q,t)\rangle \tag{18}$$

$$\frac{d^2\Sigma^{inc}}{d\Omega dE} = \frac{k}{2\pi k_o} \int_{-\infty}^{\infty} dt\exp(-i\omega t)\langle \sum_i |b_i - \langle b\rangle_i|^2 F_{ii}(Q,t)\rangle \qquad (19)$$

From equations (18) and (19) it may be seen that coherent scattering contains information on the correlations between different nuclei and hence gives information on relative spatial arrangement of atoms in the system (e.g., structure) and its time dependence. The incoherent cross section, on the other hand, contains information on correlations from the same nucleus and hence gives information on the time dependence of the motion of an individual atom (e.g., vibration, diffusion, etc.).

Because the scattering law separates into coherent and incoherent components, which may be further subdivided into elastic and inelastic and quasielastic processes, the type of information which may be obtained from neutron scattering from polymers subdivides into the general categories shown in Table II. The majority of neutron scattering experiments undertaken on polymers fall into the category of SANS for which is an example of predominantly coherent elastic scattering and the first applications of this technique to polymer science were made in the early 1970s in Europe where the first small-angle scattering cameras were developed [9]. The construction of such instruments in the U.S. began in the late 1970s at Missouri University Research Reactor (MURR), the National Bureau of Standards (NBS) and Oak Ridge National Laboratory (ORNL). In addition, a SANS spectrometer (H9B) at Brookhaven National Laboratory became operational in 1981, though this instrument is designed for small-angle structural investigations on biological materials [17], and it is on the MURR [18], NBS [19], and ORNL [20,21] instruments that the majority of SANS studies of polymers in the United States have been undertaken [9].

Table II. Information obtained from neutron scattering experiments on polymers

Type of Scattering	Energy Change		
	Elastic ($\Delta E=0$)	Quasielastic ($|\Delta E| << E_o$)	Inelastic ($\Delta E \neq 0$)
Coherent	Chain configuration in the bulk and solution (SANS), polymer compatibility (blends) Orientation mechanisms, crystal strucstructure (wide angle diffraction)	Molecular dynamics in the bulk and in solutions via Dopper broadening of the elastic peak	Elastic constants of crystalline polymer via phonon dispersion curves
Incoherent		Effective diffusion for segmental motion in the bulk activation energy	Side group vibrational frequencies and rotation barriers intermolecular potentials

HIGH CONCENTRATION LABELING

In experiments designed to determine the chain configuration in the bulk polymer by SANS, no energy discrimination is employed and the detector integrates over all energies. The scattered intensity I(Q) is measured as a function of angle and for isotropic (non-oriented) samples Q is a scalar quantity. The differential cross section is obtained by integrating equation (18) over ω and noting that this operates on the phase factor to give a delta-function in time [22]. Furthermore, for the typical elements contained in polymers the scattering lengths may be treated as real, dropping the complex conjugate, and where the element present consists predominantly of a single isotope, <b> may be replaced by b (e.g., for naturally occurring carbon $\langle b\rangle = b = 0.665 \times 10^{-12}$ cm). With these simplifications [9] equation (18) becomes

$$\frac{d\Sigma}{d\Omega}^{coh}(Q) = \langle \sum_{ij} b_i \; b_j \; \exp\,[i\underline{Q}\cdot(\underline{R}_j - \underline{R}_i)]\rangle \tag{20}$$

Nuclear cross sections have the dimensions of area, and as sample cross sections are normalized to unit volume, $d\Sigma(Q)/d\Omega$ has the dimensions of inverse length, and is typically given in units of cm^{-1}.

For a bulk polymer sample with N molecules per unit volume of pure unlabeled component we can define a coherent scattering length of a monomer unit

$$a_H = \sum_k b_k \tag{21}$$

where the summation runs over all the atoms in an unlabeled monomer unit and a similar equation may be written for the coherent scattering length of a labeled monomer unit a_D. If the two polymers are blended together so that X_H equals the mole fraction of unlabeled components and X_D is the mole fraction of the labeled polymer component the cross section is given [23,24, 25] by

$$\frac{d\Sigma}{d\Omega}(Q) = X_D \, X_H \, (a_H - a_D)^2 \, NZ^2 \, P(Q) \tag{22}$$

where P(Q) is the interchain signal which originates from monomer pairs belonging to the same polymer chain and is called the form factor of the molecule (P(0) = 1). Equation (22) is based on the assumptions that deuteration of the hydrogenous molecule has a negligible effect on the monomer-monomer interactions, and that both chains have the same polymerization index Z and the same number of molecules per unit volume (N). This shows that the scattering curve in this case is governed by the single chain form factor, P(Q). The mole fraction of each component modulates the scattered intensity with the maximum coherent scattering of the blend occurring at a 50-50 mixture of the two components. Thus P(Q) may be obtained from the measured coherent intensity at labeling levels up to 50%. Although equation (22) is essentially the same formula derived by Von Laue [26] for random binary alloys, the result was not appreciated in the earliest SANS studies of bulk polymers and concentrated solutions. These studies relied on analogies with light and x-ray scattering where the limit of zero concentration was required to eliminate interchain interference. The scattered signal was assumed to be proportional to c, the concentration (g cm^{-3}) of labeled (deuterated) polymer which has been shown to be a reasonable approximation in this limit [5,9]

$$\frac{d\Sigma}{d\Omega}(Q) = c(a_H - a_D)^2 M_{WD} \frac{N_A}{m_D{}^2} P(Q) \qquad (23)$$

where N_A is Avogadro's number, m_D is the molecular weight of a repeat unit of the deuterated polymer, and M_{WD} is the (weight-averaged) molecular weight of a deuterated chain [9].

The quantity $(a_H - a_D)^2$ is related to the difference in scattering power between labeled and unlabeled chains and is called the contrast factor. In general radiation incident on a medium whose scattering power is independent of position is scattered only into the forward direction ($2\Theta=0$). For every volume element (S) which scatters radiation through an angle $2\Theta > 0$, there is another volume element (S') which scatters exactly (180°) out of phase, and therefore all scattering cancels unless the scattering power is different at S and S', i.e., fluctuates from point-to-point in the sample. By analogy with x-ray scattering, which is caused by fluctuations in electron density, neutron scattering arises from differences in scattering length density (SLD), which is defined as the sum of coherent scattering lengths over all atoms lying in a given volume δV, divided by δV [22]. For partially labeled polymer blends the SLD is given by the coherent scattering length (equation 21) divided by the monomer volume. The coherent cross section of a system of uniform scattering length density is zero, though fluctuations may be introduced by means of isotopic substitution, thus giving rise to a finite cross section which is proportional to $(a_H - a_D)^2$. In order to produce contrast observable by x-ray scattering which can be used to give direct information on P(Q) it is necessary to change the electron density of the labeled chain. Such experiments have been performed by Hayashi et al. [27], who have labeled polystyrene chains statistically with iodine atoms and by this means concentrated solutions and bulk polymers were investigated by x-ray scattering. This type of labeling method relies on changing the chain chemistry and in general produces a greater perturbation on the chain trajectory than deuterium labeling methods. While the method seems to give reasonable results after extrapolation to infinite dilution of the iodine-labeled molecules, it seems unlikely that labeling levels of up to 50% could be used with this approach.

The contrast variation methods which have found wide application in biology can sometimes be used to remove a component of the scattering by matching its scattering power with that of the medium in which it is dispersed, and thus removing the fluctuation giving rise to the scattering. This principle is illustrated in Fig. 1, made by Professor D. Engelman of Yale University. Both tubes contain two Pyrex beads embedded in glass wool, which has a lower refractive index than the Pyrex. The tube on the left has been filled with a solvent which has the same refractive index as the glass wool. When light shines on the tubes, only the Pyrex beads are visible in the tube at left because the electron density and hence the scattering power of the glass wool has been matched with that of the solvent, thus eliminating this component of the scattering and making the wool transparent to light. In the tube at right, both the beads and glass wool scatter light, but only the glass wool can be seen because it dominates the scattering.

The parameter used to describe the overall size of a polymer chain is the radius of gyration, R_g, which may be derived from equation (22) or (23) by expanding P(Q) in a power series for low $Q(Q<R_g{}^{-1})$ and plotting $d\Sigma^{-1}(Q)/d\Omega$ versus Q^2 [5,9,23]. Alternatively these parameters may be obtained by plotting $\ln d\Sigma(Q)/d\Omega$ versus Q^2 at low Q [25,28]. These types of plots are conventionally referred to as Zimm and Guinier plots respectively and the former is generally used for investigating polymer configurations as it has been found to be linear over a wider Q-range.

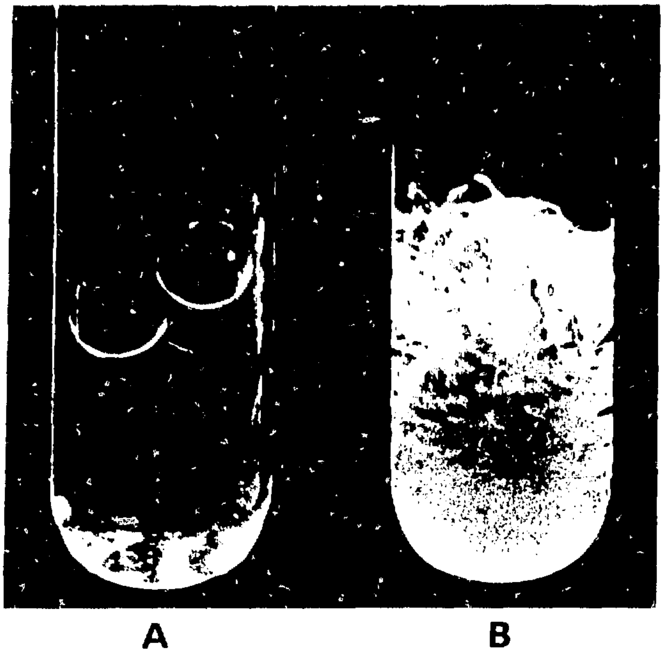

Figure 1. TWO TUBES CONTAINING PYREX BEADS IN GLASS WOOL AND SOLVENT:
A. REFRACTIVE INDEX OF SOLVENT MATCHES THAT OF GLASS WOOL.
B. REFRACTIVE INDEX OF SOLVENT IS DIFFERENT TO THAT OF GLASS WOOL OR PYREX BEADS AND SCATTERING FROM THE GLASS WOOL DOMINATES.

The first measurements in the bulk and concentrated solution were generally performed in the limit of low relative labeling and extrapolated to zero concentration. In this range

$$\frac{d\Sigma^{-1}}{d\Omega}(Q) = \frac{m_D^2}{c(a_H-a_D)^2 M_{wD} N_A}\left[1 + \frac{Q^2R_g^2}{3} + ..\right] \qquad (24)$$

and thus R_g and M_{wD} may be derived from the slope and Q=0 intercept of such a plot [9]. The realization that the same information could be obtained with greater accuracy at much higher levels of labeling was made [24,29-31] and verified independently by several groups [23,29-33]. Figure 2 shows the variation of R_g with the concentration of labeled molecules in amorphous polycarbonate [33] and shows that the measured values are independent of the level of labeling. Similarly Fig. 3 shows that the extrapolated Q=0 cross section, $d\Sigma(0)/d\Omega$, is proportional to the product, X_HX_D, for amorphous polystyrene [23] as expected from equation (22). This equation was derived on assuming equal polymerization indices for the labeled and unlabeled chains. The effect of unequal indices has been considered by Boué et al., [34] who showed how the measured R_g and $d\Sigma(0)/d\Omega$ were perturbed by this mismatch. In this case the mole fractions X_D, X_H in equation (22) are replaced by volume fractions Φ_D, Φ_H (9,34).

AMORPHOUS POLYMERS

The first convincing demonstration of the power of the SANS technique was made in the field of bulk amorphous polymers. It is well known that there have been several theoretical approaches to the molecular conformation in these systems, based on the unperturbed Gaussian (random) coil due to Flory and co-workers [35,36] and the meander or bundle models [37-38] where

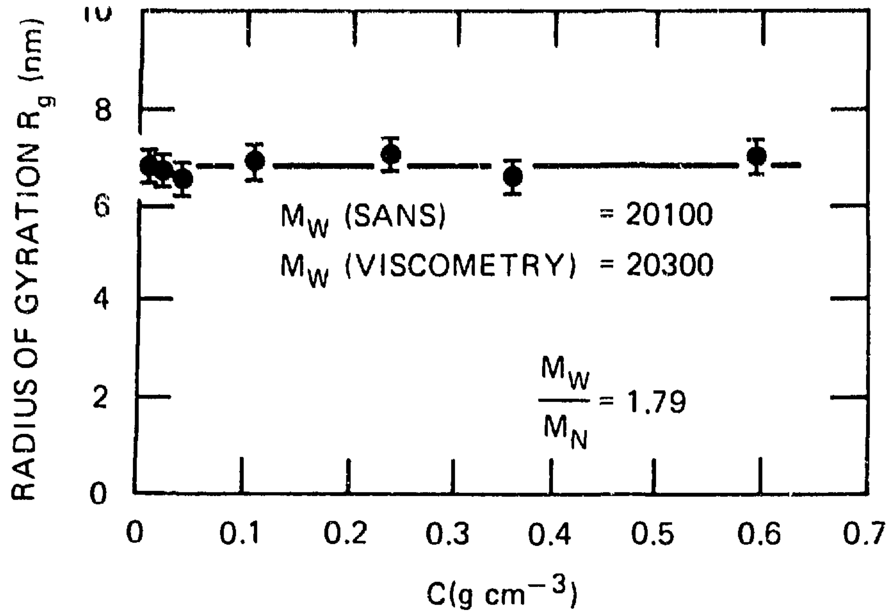

Figure 2. RADIUS OF GYRATION, R_g, FOR MOLECULES IN AMORPHOUS POLYCARBONATE VERSUS THE CONCENTRATION OF LABELED(DEUTERATED) POLYMER

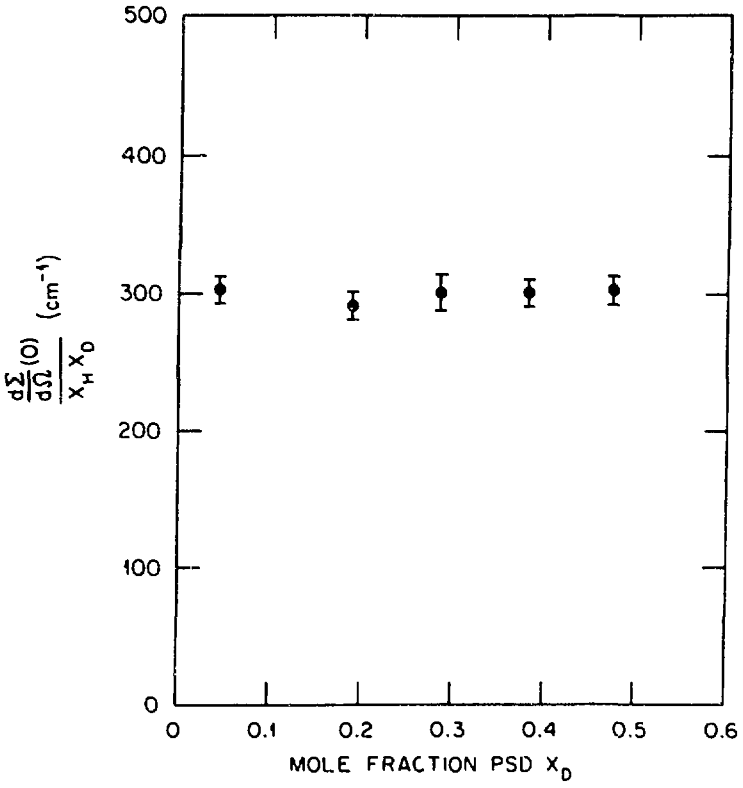

Figure 3. Variation of $\frac{1}{X_H X_D} \frac{d\Sigma}{d\Omega}(0)$ with X_D for Blends of Deuterated and Normal (Hydrogenous) Polystyrene.

arrangement. In addition a collapsed coil model was advanced for some systems [39]. Before the development of the SANS technique there was no way of directly measuring the molecular configuration in bulk polymers and this led to intense debate on the issue in the literature. To the author's knowledge, the first suggestion to use the contrast between deuterated and normal (hydrogenous) molecules to provide a direct determination of P(Q) was made independently in at least two groups [40,41] in the late 1960s and the method was first demonstrated in principle in the early 1970s [42-49].

According to the random coil model, R_g^w should be proportional to $M_w^{1/2}$, where M_w is the (weight averaged) molecular weight, with the same constant of proportionality in the bulk as in an ideal Θ-solvent. It may be seen from Table III that in general this prediction holds remarkably well for amorphous polymers and that there is close agreement between data on the same polymer studied independently by different groups.

While these results have given impressive support to this model they are not in themselves conclusive, since it was subsequently shown for crystalline polymers that R_g is very similar for molecules in the molten (amorphous) and solid (crystalline) states. Thus the finding that molecules exhibit the unperturbed dimensions in the molten or glassy amorphous state does not in itself rule out significant parallelism for an appreciable fraction of the molecules. In order to test how far the local molecular conformation, as opposed to the overall R_g is described by the various models,

Table III. Molecular dimensions in bulk amorphous polymers

Polymer	State	$[(R_g^w)^2/M_w]^{1/2}$ (Å $g^{-1/2}$)		Reference
		Bulk	Θ-Solvent	
Poly(methyl methacrylate) (Atactic)	Glass	0.27	0.25	43-44
Polystyrene (Atactic)	Glass	0.280	0.275	45
Polystyrene (Atactic)	Glass	0.275	0.275	46
Polystyrene (Atactic)	Melt	0.280	0.275	47
Polyethylene	Melt	0.45	0.45	48
Polyethylene	Melt	0.46	0.45	49
Poly(vinyl chloride)	Glass	0.40	0.37	50
Polyisobutylene	Glass	0.31	0.30	51
Poly(ethylene terepthalate)	Glass	0.39	0.39-0.42	52
Poly(methyl methacrylate) (atactic)	Glass	0.25	0.25	53
(Syndiotactic)	Glass	0.29	0.24	
(Isotactic)	Glass	0.30	0.28	
Polybutadiene	Melt	0.35	0.34-0.42	54

measurements have been extended to higher values of Q. To first order the scattered intensity at a given Q is sensitive to fluctuations in the scattering length density on a distance scale $D \sim 2\pi/Q$ and thus as Q increases the scattering is increasingly determined by the local chain conformation. This may be calculated for the random coil model using rotational isomeric statistics [36] and hence the scattered intensity may be estimated numerically and compared with experiment. This is accomplished by measuring the scattering in the intermediate angle range ($0.1 < Q < 0.6$ A^{1}) which is sensitive to the local conformation of the chain over distances ~10-50 A. Figure 4 shows intermediate angle neutron scattering (IANS) data for molten polyethylene [49] at T = 150°C compared to the rotational isomeric state (RIS) calculation of Yoon and Flory [55] and the Debye model for a coil with a Gaussian distribution of chain elements [56,57]. The data are plotted as $Q^2 \, d\Sigma(Q)/d\Omega$ vs Q as used by Kratky [58] since this representation enhances the scattering at higher Q and facilitates comparison with different models. It may be seen from Fig. 4, that $d\Sigma(Q)/d\Omega$ varies as Q^{-2} in this region leading to a plateau in the Kratky plot, which is closely fitted by both the RIS calculation and Gaussian coil function. Similarly the IANS data for atactic polystyrene are consistent with the Debye model both in the melt and glassy states [46,47]. Similar comparisons in the intermediate Q-range have also been made with polyisobutylene [51], poly(methyl methacrylate) [53] and polycarbonate [59] and in each case reasonable agreement was achieved with the rotational isomeric theory. To the author's knowledge there are no major discrepancies between theory and the scattering experiments which might be indicative of quasiparallel packing of polymer chains.

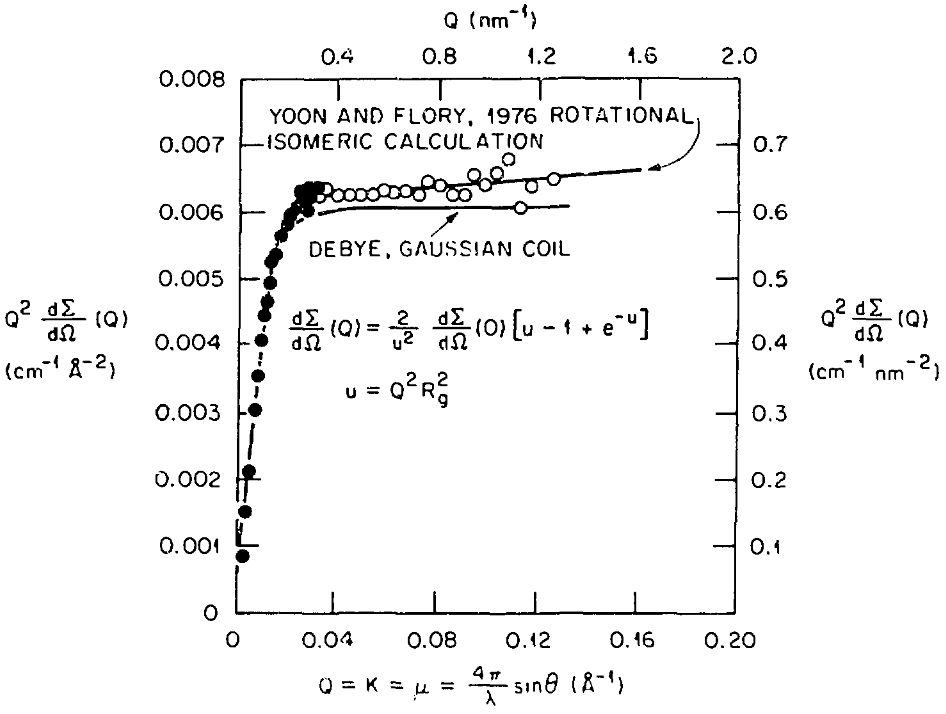

Figure 4. KRATKY PLOT FOR MOLTEN POLYETHYLENE AT 150°C

The arrangement of molecular chains within the lamellae of semicrystalline polymers has long been disputed [60-63] and SANS has provided new information on this subject. It is generally agreed that semicrystalline polymers exhibit a lamellar morphology both for material crystallized from the melt and from dilute solution. The thickness of lamellae is typically 100-500 A with amorphous polymer interspersed between the crystalline regions. The molecular chains are at an angle (0-30°) to the lamellar normals and have lengths much greater than the lamellar thickness, thus traversing one or more lamellae several times. Based on considerations of density conservation at the crystal-amorphous boundary, Flory [60] demonstrated that a considerable fraction (~0.5) of chains must return to the same crystal. What is in question is, whether the molecule returns with predominantly adjacent or with random reentry to the crystallite of origin.

Generally the SANS experiments reveal that the radius of gyration, R_g of molecules remains unchanged upon crystallization from the melt [9,29, 48,49,64,65] and hence has a $M^{1/2}$ dependence in both the molten and crystalline states. This indicates that the molecules crystallize with a similar distribution of mass elements to that possessed in the melt [49] and hence is distributed over several lamellae in the crystalline state. For solution-crystallized material, however, the radius of gyration is relatively independent of molecular weight, and is generally markedly reduced from the dimensions in dilute solutions [66,67] indicating a much more compact configuration. These measurements of R_g were made at low Q and contain no information on the mutual arrangement of stems i.e., straight sections of a chain traversing a crystalline lamella. This is best examined by experiments in the intermediate angle range which is sensitive to the correlation of stems over distances 10-50 A. This type of measurement has been made for several systems [49,67-70] and compared with a variety of model calculations which simulate the chain trajectory [49,59,67-75]. Fig. 5 shows IANS data [59b] for polyethylene quench crystallized from the melt where the scattering function $F_n(Q)$ is defined by

$$F_n(Q) = (n+1)Q^2 P(Q) = (n+1)Q^2 \frac{\frac{d\Sigma}{d\Omega}(Q)}{\frac{d\Sigma}{d\Omega}(0)} \qquad (25)$$

and n is the number of bonds in the chain.

There is reasonable consistency between the data from several groups [49,67-69] which is compared with model calculations based on Monte Carlo statistics as a function of the probability (p_{ar}) that the stem will fold adjacently along the (110) plane [59]. It may be seen that the model leads to a Q^{-2} dependence for $d\Sigma(Q)/d\Omega$ and hence a plateau in the Kratky plot. The plateau levels differ by a factor ~2 for the extremes of random ($p_{ar} = 0$) and adjacent ($p_{ar} = 1$) reentry and it was concluded [49,74] that the IANS data were inconsistent with regular folding. Similar model calculations have also been performed as a function of the number of stems folded adjacently in a central cluster [73]. It was concluded that this model could fit the neutron data with higher probabilities (~0.7) of adjacent folding, though this involved plotting the experimental data [49] as a function of the molecular weight of the labeled chains, measured by both SANS (M_w = 46000) and chromatographic techniques (M_w = 60,000). In the opinion of the author and others [69] this procedure introduces unnecessary uncertainty into the height of the plateau level in $F_n(Q)$ and hence makes the comparison less precise. It may be seen from equation (25) that for high molecular weight material (n>1000), $F_n(Q)$ is independent of molecular weight to a very good approximation, since $d\Sigma(0)/d\Omega$ contains the molecular weight which is proportional to n. This parameter may therefore be canceled thus making

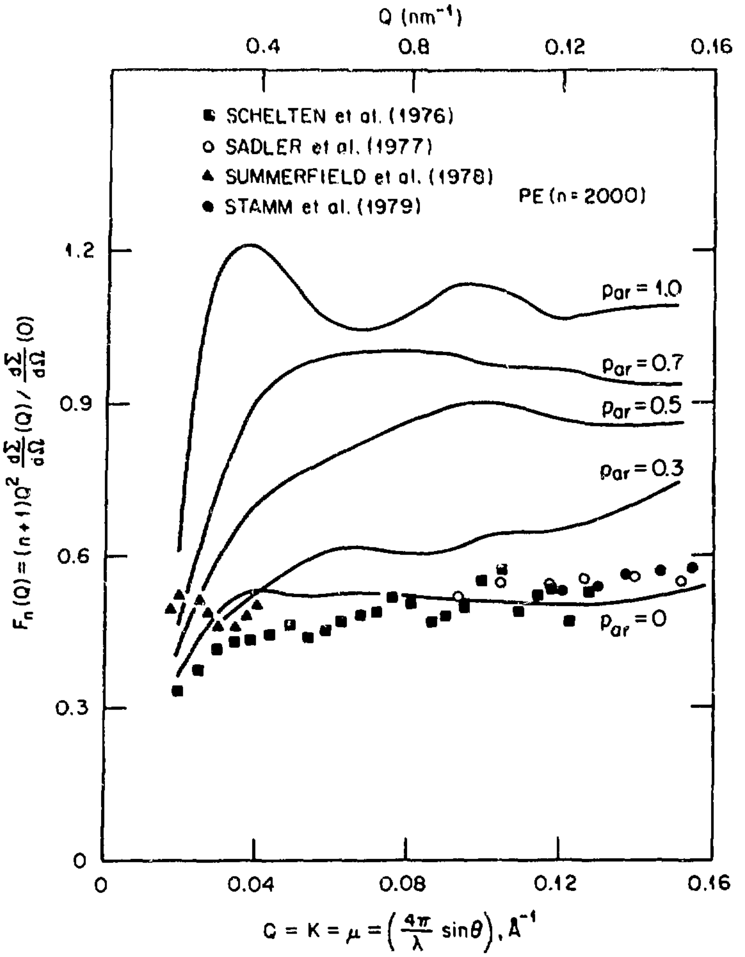

Figure 5. CALCULATION OF $F_n(Q)$ AS A FUNCTION OF THE PROBABILITY OF ADJACENT FOLDING (p_{ar})

$F_n(Q)$ independent of molecular weight, and this would lead to a lower estimate of the number of stems in a central cluster or the probability of adjacent folding.

In a careful review of the scattering from both quenched and slow cooled materials Sadler [76] concluded that the degree of adjacency within the rows is ~30-50% for melt grown crystals and while the precise definition of p_{ar} varies between different models, it seems that probabilities of this order are inconsistent with regular folding of an appreciable number (>4) of stems in one crystallographic plane. Longer sequences of adjacent stems would lead to an observable modulation of the wide angle neutron scattering pattern ($Q>6\ nm^{-1}$) as pointed out by Stamm [77], and such modulations are not observed for melt crystallized polyethylene [77,78]. However, it was pointed out by Guttman et al. [73] that a larger proportion of folds were relatively close, and that the folds which were not adjacent are 'near' and rarely involved stem separations greater than three nearest neighbors. This is also consistent with estimates of the distribution of distances of reentry made using a method proposed for the evaluation of neutron scattering data independently of detailed structural models [79,80]. The only assumption of this approach is that the molecular structure can be described as consisting of 'clusters' of stems belonging to the same molecule in each lamella. The analysis leads to the average number of clusters per molecule, N_c, the radius of gyration of the centers of stems belonging to one cluster $\langle R_{cc}^2\rangle^{1/2}$, and the average number of tie molecules per chain. The analysis has been applied to melt crystallized polyethylene [79], polypropylene [79] and poly(ethylene oxide) [80]. Typical values of N_c are in the range 4-13, whereas, $\langle R_{cc}\rangle^{1/2}$ is of the order 15-60 A. The average distance between stems $\langle a\rangle$ may be derived from $\langle R_{cc}\rangle^{1/2}$ on the assumptions of a random walk or a linear arrangement of stems (regular folding). On the latter assumption the values of $\langle a\rangle$ are 2-3 times greater than the distances involved in regular folding in one crystallographic plane ($\langle a\rangle \sim 5$ A). Assuming a random walk, values of $\langle a\rangle$ are in the range 20-40 A which is consistent with the conclusion of 'near' but not adjacent folding following from the above model calculations. Futher details of comparisons with model calculations for both melt and solution crystallized materials are given in reference [9]. While some significant disagreement still persists and further work is in progress, it seems generally agreed that the neutron data rules out the possibility that a typical molecule is regularly folded in one crystallographic plane over many stems without interruption. This model had gained widespread support over the previous decades for both melt and solution crystallized material. Similarly the extremes of random configurations have been ruled out with a large fraction of molecules usually folding in 'near' reentry within a few nearest neighbors.

As mentioned earlier, the above studies of polymer blends are based on the assumption that the interactions are independent of deuteration, or alternatively that the interaction parameter between labeled and unlabeled molecules of the same species, χ_{HD}, is zero. This assumption has also been implicit in all previous SANS studies though calculations [82] have indicated that χ_{HD} may be finite and of the order of 10^{-4}-10^{-3}. This has led to the suggestion [83] that for sufficiently high molecular weights, demixing could occur in mixtures of deuterated and hydrogenous molecules of the same species, and that this could lead to the measurement of $_{HD}$. Such experiments have been performed by Bates et al. [84,85] who examined binary mixtures of deuterium labeled and unlabeled 1-4 polybutadienes. By regarding the labeled and unlabeled molecules as different species with volume fractions ϕ_H and ϕ_D, the interaction parameter χ_{HD} between them may be estimated by fitting the equation random phase approximation (RPA) of deGennes [83-85] to the measured scattering data.

Figure 6 shows a plot of χ_{HD} as a function of inverse temperature, T^{-1} (K^{-1}) which reaches the value on the spinodal at $T_S = 242.1 \pm 0.7$ K. The critical exponents exhibited the mean field values and at room temperature (T=296 K) the value of $\chi_{HD} = 8.8 \times 10^{-4}$. Similar measurements in binary mixtures of deuterated and protonated polystyrenes [85] and poly (dimethyl-siloxanes) [86] corroborate the prediction of a universal isotope effect, which has been shown to be a consequence of zero-point motion in conjunction with the anharmonicity of the interatomic potential [87]. Since χ values of the order 10^{-4}-10^{-3} are in general much smaller than the values measured between different species it does not invalidate the methods described for the measurement of χ in polymer blends [25]. However, the correction for this effect must be considered in measurements of smaller parameters. Similarly the effect of a finite χ_{HD} does not invalidate the vast majority of investigations using the SANS techniques as segregation effects are important only in high molecular weight systems and have generally not been observed. However the effect of a finite χ_{HD} on measurements of interdiffusion constants of polystyrene has already been measured [88] and the magnitude of the effect is consistent with the values of χ_{HD} determined for this system [85].

The above examples along with others given in this Symposium [25,89,90] are indicative of the information which can be gained on structure on the distance scale 10-1000 A by small-angle scattering techniques. When combined with deuterium labeling, SANS can give further unique information polymer chain configuration in a wide variety of polymer systems [9].

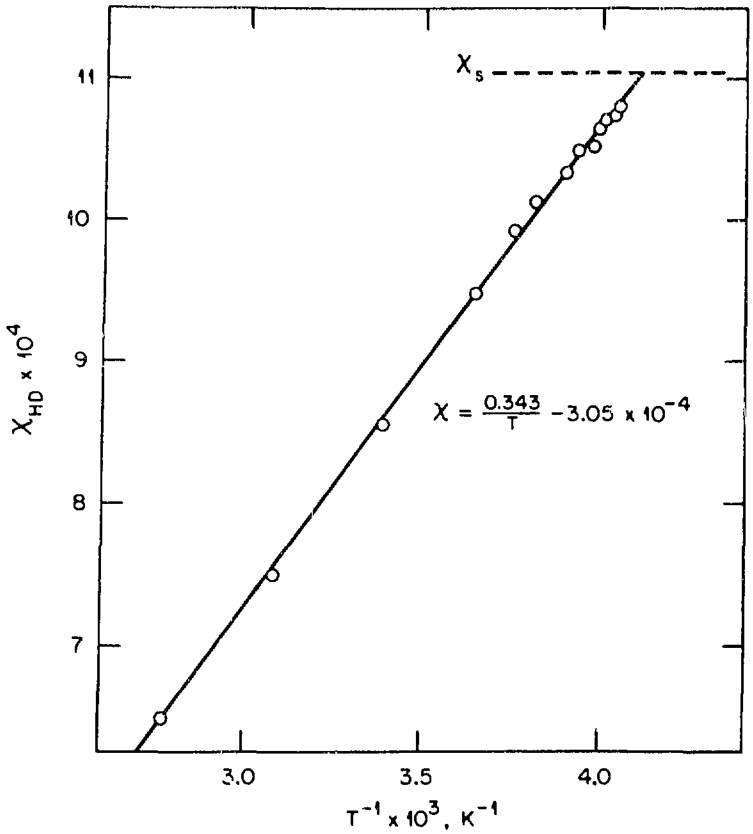

Figure 6. PLOT OF X_{HD} VERSUS T^{-1} FOR BLEND OF DEUTERATED ($\phi_D = 0.31$) AND HYDROGENOUS ($\phi_H = 0.69$) POLYBUTADIENES

ACKNOWLEDGEMENT

Research sponsored by the National Science Foundation Grant No. DMR-7724459 through Interagency Agreement No. 40-636-77 with the U.S. Department of Energy under contract DE-AC05-84OR21400 with Martin Marietta Energy Systems, Inc.

REFERENCE

1. V. E. Turchin, Slow Neutrons, Israel Program for Scientific Translations, Jerusalem, 1965.
2. H. Boutin and S. Yip, Molecular Spectroscopy with Neutrons, MIT Press, Cambridge, Mass, 1968.
3. G. E. Bacon, Neutron Diffraction, Clarendon Press, Oxford, England, 1971.
4. W. Marshall and S. W. Lovesey, Theory of Thermal Neutron Scattering, Clarendon Press, Oxford, England, 1971.
5. A. Maconnachie and R. W. Richards, Polymer 19, 739 (1978).
6. J. S. Higgins in G. Kostorz, ed., Treatise on Materials Science and Technology, Academic Press, New York, 15, 381 (1979).
7. L. H. Sperling, Polymer Engineering and Sci. 24, 1 (1984).
8. J. S. Higgins and R. S. Stein, J. Appl. Cryst. 11, 346 (1978).

9. G. D. Wignall, "Neutron Scattering from Polymers," in Encyclopedia of Polymer Science and Engineering, 2nd Edition, ed. by Martin Grayson and Jacqueline I. Kroschwitz, John Wiley and Sons, New York, 1986 (in press).
10. G. D. Wignall and F. S. Bates, J. Appl. Cryst. (in press).
11. L. I. Schiff, Quantum Mechanics, McGraw-Hill, New York, 1955.
12. C. G. Windsor, in B.T. M. Willis, ed., Chemical Applications of Thermal Neutron Scattering, Oxford University Press, London, England, 1973.
13. W. M. Lomer and G. G. Low, in P. A. Egelstaff, ed., Thermal Neutron Scattering, Academic Press, New York, 1965, Chapter 1.
14. J. A. Janik and A. Kowalska, in P. A. Egelstaff, ed., Thermal Neutron Scattering, Academic Press, New York, 1965, Chapter 10.
15. Neutron Cross Sections, D. I. Garber and R. R. Kinser, eds., Brookhaven National Laboratory, BNL325, 3rd Ed., Upton, New York, 1976; BNL 325, 2nd Edition Supplement No. 2, 1964.
16. A. Maconnachie, Polymer 25, 1068 (1984).
17. B. P. Schoenborn, D. S. Wise, and D. K. Schneider, Trans. Amer. Cryst. Assoc. 19, 67 (1983).
18. D.F.R. Mildner, R. Berliner, O. A. Pringle, and J. S. King, J. Appl. Cryst. 14, 370 (1981).
19. C. Glinka in J. Faber, ed., Amer. Inst. of Phys. Conf. Proc. no. 89, 395 (1982).
20. W. C. Koehler, R. W. Hendricks, H. R. Child, S. P. King, J. S. Lin, and G. D. Wignall, in S. H. Chen, B. Chu, and R. Nossal, eds., Scattering Techniques Applied to Supramolecular and Nonequilibrium Systems, Plenum Press, New York, NATO Advanced Study Series 83, 35 (1981).
21. W. C. Koehler, Physica 137B, 320 (1986).
22. J. B. Hayter in V. Degiorgio and M. Corti, eds., Proceedings of Enrico Fermic School of Physics Course XC, Amsterdam (1985), p. 59.
23. G. D. Wignall, R. W. Hendricks, W. C. Koehler, J. S. Lin, M. P. Wai, E.L.T. Thomas, and R. S. Stein, Polymer 22, 886 (1981).
24. This result was developed by R. S. Stein (1980) following an earlier suggestion by H. Benoit (1980) and was published in reference 23. Similar derivations were given independently in references 29-31.
25. R. S. Stein, see article in this volume.
26. M. Von Laue, Ann. Phys. 56, 497 (1918).
27. H. Hayashi, F. Hamada, and A. Nakajima, Macromolecules 9, 543 (1976).
28. A. Guinier and G. Fournet, Small-Angle Scattering of X-Rays, John Wiley, New York, (1955).
29. E. W. Fischer, M. Stamm, M. Dettenmaier, and P. Herschenroeder, Polymer Preprints 20(1), 219 (1979).
30. C. E. Williams et al., J. Polym. Sci., Polym. Lett. Ed. 17, 379 (1979).
31. A. Z. Akcasu, G. C. Summerfield, S. N. Jahshan, C. C. Han, C. Y. Kim, and H. Yu, J. Polym. Sci. 18, 865 (1980).
32. (a) Tangari, G. C. Summerfield, J. S. King, R. Berliner, and D.F.R. Mildner, Macromolecules 13, 1546 (1980); (b) C. Tangari, J. S. King, and G. C. Summerfield, Macromolecules 15, 132 (1982).
33. W. Gawrisch, M. G. Brereton, and E. W. Fisher, Polymer Bull. 4, 687 (1981).
34. F. Boué, M. Nierlich, and L. Leibler, Polymer 23, 29 (1982).
35. P. J. Flory, J. Chem. Phys. 17, 303 (1949); P. J. Flory, Principles of Polymer Chemistry, Cornell University Press, (1953), p. 426.
36. P. J. Flory, Statistical Mechanics of Chain Molecules, John Wiley-Interscience, New York and London (1968), p. 34.
37. W. R. Pechhold, Kolloid Z 228, 1 (1968).
38. (a) G.S.Y. Yeh, Rev. Macromol. Sci. 1, 173 (1972); (b) G.S.Y. Yeh and P. H. Geil, J. Macromol. Sci. (Phys.) B1(2), 235 (1967).
39. A. Kampf, M. Hoffman, and H. Kramer, Ber. Bunsenges 74, 851 (1970).
40. R. G. Kirste, Jahresbericht 1969 des Sonderforschungsbereiches, Mainz 41, 547 (1970).

41. G. D. Wignall, Imperial Chemical Industries (Runcorn), Memo PPR G19 (1970).
42. J. P. Cotton, B. Farnoux, G. Jannink, J. Mons, and C. Picot, C. R. Acad. Sci. (Paris) 275, 3C, 175 (1972).
43. (a) R. G. Kirste, W. A. Kruse, and J. Schelten, J. Makromol. Chem. 162, 299 (1972); (b) Koll. Z. Z Polym. 251, 919 (1973).
44. R. G. Kirste, W. A. Kruse, and K. Ibel, Polymer 16, 120 (1975).
45. D.G.H. Ballard, G. D. Wignall and J. Schelten, Eur. Polym. J. 9, 965 (1973).
46. H. Benoit, J. P. Cotton, D. Decker, B. Farnoux, J. S. Higgins, G. Jannink, R. Ober, and C. Picot, Nature 245, 23 (1973).
47. G. D. Wignall, D.G.H. Ballard, and J. Schelten, Eur. Polym. J. 10, 861 (1974).
48. G. Lieser, E. W. Fischer and K. Ibel, J. Polym. Sci. 13, 29 (1975).
49. J. Schelten, D.G.H. Ballard, G. D. Wignall, G. Longman, and W. Schmatz, Polymer 27, 751 (1976).
50. P. Herschenroeder, Thesis, Mainz (1978).
51. H. Hayashi, P. J. Flory, and G. D. Wignall, Macromolecules 16, 1328 (1983).
52. K. P. McAlea, J. M. Schultz, K. H. Gardner, and G. D. Wignall, Macomolecules 18, 477 (1985).
53. J. M. O'Reilly, D. M. Teegarden, and G. D. Wignall, Macromolecules 18, 2747 (1985).
54. A. M. Fernandez, L. H. Sperling, and G. D. Wignall, Macromolecules 19, 2572 (1986).
55. D. Yoon and P. J. Flory, Macromolecules 9, 294 (1976).
56. P. Debye, J. Appl. Phys. 15, 338 (1944).
57. P. J. Flory, Principles of Polymer Chemistry, Cornell University Press p. 295, 1969.
58. O. Kratky, Koll. Z. 182, 7 (1962).
59. (a) D. Y. Yoon and P. J. Flory, Polym. Bull. 4, 692 (1981); (b). P. J. Flory, Pure and Applied Chem. 56, 305 (1984).
60. P. J. Flory, J. Am. Chem. Soc. 84, 2857 (1962).
61. E. W. Fischer and R. Lorenz, Kolloid Z. 189, 97 (1963).
62. A. Keller, Philos. Mag. 2, 1171 (1957); Makromol. Chem. 34, 1 (1959).
63. J. D. Hoffman and J. L. Laurizen, J. Res. Natl. Bur. Stand. Sect. A, 65A, 297 (1961).
64. D.G.H. Ballard, P. Cheshire, G. W. Longman, and J. Schelten, Polymer 19, 379 (1978).
65. J. M. Guenet, Polymer 22, 313 (1981).
66. D. M. Sadler and A. Keller, Science 19, 265 (1979).
67. D. M. Sadler and A. Keller, Macromolecules 10, 1128 (1977).
68. G. C. Summerfield, J. S. King, and R. Ullman, J. Appl. Cryst. 11, 548 (1978).
69. M. Stamm, E. W. Fischer, M. Dettenmaier, and P. Convert, Discuss. Faraday Soc. 68, 263 (1979).
70. M. Stamm, J. Schelten, D.G.H. Ballard, Colloid and Polym. Sci. 259, 286 (1981).
71. D. Y. Yoon and P. J. Flory, Discuss. Faraday Soc. 68, 288 (1980).
72. J. D. Hoffman, C. M. Guttman, and E. A. Dimarzio, Discuss. Faraday Soc. 68, 177 (1979).
73. C. M. Guttman, J. D. Hoffman and E. A. Dimarzio, Discuss. Faraday Soc. 68, 197 (1979); Polymer 22, 597 (1981).
74. P. J. Flory and D. Y. Yoon, Nature 272, 226 (1977).
75. D. M. Sadler, and R. Harris, J. Polym. Sci., Polym. Phys. Ed. 20, 561 (1982).
76. D. Sadler in I. Hall, ed., The Structure of Crystalline Polymers, Applied Science Publisher, (1983), p. 125.
77. M. Stamm, J. Polym. Sci., Polym. Phys. Ed., 20, 235 (1982).

Start here

78. G. D. Wignall, L. Mandelkern, C. Edwards, and M. Glotin, J. Polym. Sci., Polym. Phys. Ed. 20, 245 (1982).

79. E. W. Fischer, K. Hahn, J. Kugler, and R. Bom, J. Polym. Sci., Polym. Phys. Ed. 22, 1491 (1984).

80. E. W. Fischer, Polym. J. 17, 307 (1985).

81. S. J. Spells and D. M. Sadler, Polymer 25, 739 (1984).

82. A. B. Buckingham and H.G.E. Hentschel, J. Poly. Sci., Polym. Phys. Ed. 18, 853 (1980).

83. P. G. deGennes, Scaling Concepts in Polymer Physics, Cornell University Press, New York, 1979, Chapter IV.

84. F. S. Bates, G. D. Wignall, and W. C. Koehler, Phys. Rev. Lett. 55, 2425 (1985).

85. F. S. Bates and G. D. Wignall, Macromolecules 19, 932 (1986).

86. A. Lapp, C. Picot, and Benoit, Macromolecules 18, 2437 (1985).

87. F. S. Bates and G. D. Wignall, Phys. Rev. Lett. 57, 1429 (1986).

88. P. Green and B. L. Doyle, Phys. Rev. Lett. 57, 1407 (1986).

89. D. W. Schaefer, see article in this volume.

90. R. J. Roe, see article in this volume.

DISCLAIMER

This report was prepared as an account of work sponsored by an agency of the United States Government. Neither the United States Government nor any agency thereof, nor any of their employees, makes any warranty, express or implied, or assumes any legal liability or responsibility for the accuracy, completeness, or usefulness of any information, apparatus, product, or process disclosed, or represents that its use would not infringe privately owned rights. Reference herein to any specific commercial product, process, or service by trade name, trademark, manufacturer, or otherwise does not necessarily constitute or imply its endorsement, recommendation, or favoring by the United States Government or any agency thereof. The views and opinions of authors expressed herein do not necessarily state or reflect those of the United States Government or any agency thereof.